orientations. It appears that the restrictions for CO binding in *Thyonella* hemoglobin must be even more severe.

References

Adair, G. S. (1925) *J. Biol. Chem. 63*, 529.
Becsey, J. G., Berke, L., & Callan, J. R. (1968) *J. Chem. Educ. 45*, 728.
Edelstein, S. J., Rehmer, M. J., Olson, J. S., & Gibson, Q. H. (1970) *J. Biol. Chem. 245*, 4372.
Geraci, G., Parkhurst, L. J., Sada, A., & Cirotto, C. (1977) *Myoglobin, Colloq., 1976*, 75.
Gibson, Q. (1959a) *Discuss. Faraday Soc. 27*, 142.
Gibson, Q. (1959b) *Biochem. J. 71*, 293.
Heidner, E. J., Ladner, R. C., & Perutz, M. F. (1976) *J. Mol. Biol. 104*, 707.
LaGow, J., & Parkhurst, L. J. (1972) *Biochemistry 11*, 4520.
Monod, J., Wyman, J., & Changeux, J.-P. (1965) *J. Mol. Biol. 12*, 88.
Parkhurst, L. J., & Gibson, Q. H. (1967) *J. Biol. Chem. 242*, 5762.
Sawicki, C. A., & Gibson, Q. H. (1977) *J. Biol. Chem. 252*, 5783.
Sharma, V. S., Ranney, H. M., Geibel, J. F., & Traylor, T. G. (1975) *Biochem. Biophys. Res. Commun. 66*, 1301.
Steinmeier, R. C., & Parkhurst, L. J. (1975) *Biochemistry 14*, 1564.
Steinmeier, R. C., & Parkhurst, L. J. (1979) *Biochemistry* (preceding paper in this issue).
Yang, M. C. (1974) Ph.D. Thesis, University of Nebraska, Lincoln, NB.

Nuclear Magnetic Resonance Conformational Studies on the Chemotactic Tripeptide Formyl-L-methionyl-L-leucyl-L-phenylalanine. A Small β Sheet†

E. L. Becker, H. E. Bleich, A. R. Day, R. J. Freer, J. A. Glasel,* and J. Visintainer

ABSTRACT: Previous work by several groups has shown that the combination of spin–spin coupling constants and spectral density components (derived from spin–lattice relaxation and/or nuclear Overhauser measurements) may aid in the task of conformational determination of peptides in solution. Using the peptide formyl-L-methionyl-L-leucyl-L-phenylalanine, which is a potent specific chemotactic agent for leucocytes, we show the following: (a) that $^3J_{NHCH}$ coupling constants are consistent with a high degree of rigidity in the peptide backbone in solution, (b) that ^2H isotopic substitution in combination with relaxation data taken at different Larmor frequencies enables spectral density, and thence conformational, information to be obtained, (c) that side-chain conformations for this molecule mirror, in some aspects, those found in the solid state for other peptides containing the same residues, and (d) that temperature dependence of amide chemical shifts does not have direct implication concerning the existence of intramolecular hydrogen bonds in peptides. We are able to propose a family of conformations which appear to interchange rapidly on the NMR time scale and are characterized by a distribution of side-chain rotamers. The basic backbone conformation is, or closely approximates, a small β antiparallel pleated sheet and as such suggests a possible mode of receptor–chemotactic peptide interaction.

The phenomenon of leucocyte chemotaxis, that is, the directed motion of leucocytes along a concentration gradient of certain substances, has occupied the attention of pathologists and immunologists for many years. Historically, a large number of substances have been observed to cause chemotactic behavior in neutrophil leucocytes (Wilkinson, 1974). However, recently interest has focused on small peptides as chemotactic factors. Indeed, recently it was found that several formylated methionyl peptides show chemotactic behavior (Schiffman et al., 1975). Further work (Showell et al., 1976) has shown, via extensive structure–activity peptide synthesis, that the tripeptide CHO-Met-Leu-Phe-OH is a specific chemotactic factor for neutrophil leucocytes. These cells are sensitive to the tripeptide in amounts less than 2400 molecules of peptide per cell. Additional work (Aswanikumar et al., 1977) has shown that the interaction of the peptide with neutrophil cells is via specific receptors. Structure–activity studies have shown strict correlation between covalent structural changes in the peptide and the rank order of pharmacological activity seen in four assay procedures (Showell et al., 1976; Day et al., 1977). This group of peptides is therefore of particular importance since it represents a means of studying cellular immune responses by using a well-defined pure material in contrast to ill-defined chemotactic "factors" of unknown composition (Wilkinson, 1974).

Because of its simplicity and the future possibility of isolating receptor apparatuses from neutrophils, it is clear that this tripeptide is a good system to try to apply contemporary methods involving through-bond and through-space measurements as far as gathering information on its solution

† From the Departments of Pathology (E.L.B.) and Biochemistry (H.E.B., J.A.G., and J.V.), University of Connecticut Health Center, Farmington, Connecticut 06032, and the Department of Pharmacology (A.R.D. and R.J.F.), Medical College of Virginia, Richmond, Virginia 23298. *Received February 20, 1979.* This work was supported by National Institutes of Drug Research Contract DE-62494 (R.J.F.), National Institutes of Health Grant AI09648 (E.B.), National Science Foundation Grant PCM 78-08543, and National Institutes of Health Grant RR00639 (J.A.G.)

* The authors of this work are given alphabetically. The areas of responsibility for the three laboratories involved are as follows: NMR experiment and theory (J.A.G.); biological (E.L.B.) and peptide synthesis (R.J.F.).

0006-2960/79/0418-4656$01.00/0

Scheme I

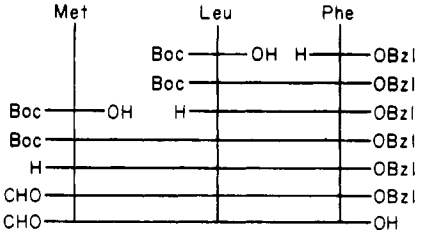

conformational dynamics is concerned.

Over the past decade a considerable effort has been devoted to the end of determining accurate peptide conformations via nuclear magnetic resonance (NMR) spectroscopy. For the case of small cyclical peptides, this work has now reached a level where a good deal of confidence may be placed in the conformational conclusions derived from empirical results (Bystrov et al., 1978). Unfortunately, from a biological standpoint, that class of peptides contains relatively few examples and those are with rather ill-defined receptors. On the other hand, the present time is one in which new, open chain peptides with profound biological activities are continually being found by neurochemists, physiologists, pharmacologists, and immunologists who would like to relate solution and receptor conformation to biological activity. Many of this latter class of peptides have relatively abundant, and increasingly well-defined, receptor systems. However, it is very doubtful that the same techniques which are now being used successfully to determine cyclic peptide conformation are applicable to those with open chains. The reason is simply that the methods currently in use depend upon ring closure to prevent additive errors in the sets of derived torsional angles which define peptide conformations. Therefore, an effort has been mounted in recent years to develop NMR methods which use through-space effects to help define peptide conformations.

Experimental Procedures

Experimental Methods

Peptide Synthesis. The primary structure of amino acids in FMLP[1] is shown in Figure 1, together with the nomenclature (IUPAC–IUB Commission, 1970) used for the main- and side-chain angles in the molecule.

The peptide was synthesized according to Scheme I (Day & Freer, 1979) by using a modification of the mixed anhydride procedure of Tilak (Tilak, 1970). The final product was crystallized from acetone.

NMR Sample Preparation. As previously described, great care was taken to eliminate the well-known effects of introduced paramagnetic impurities and dissolved oxygen upon relaxation times (Bleich et al., 1976). The crystalline peptide resulting from the synthetic procedure described above was brought to pH 8 with NaOH in doubly glass-distilled H_2O, lyophilized, and then dried overnight in vacuo over P_2O_5 at 50 °C. Dissolved oxygen was removed from the NMR solvent dimethyl-d_6 sulfoxide (Me_2SO-d_6) (100% isotopic enrichment for ^1H; 99.5% for ^{13}C) via four freeze–pump–thaw cycles. The experiments described were therefore on the negatively charged form of FMLP dissolved in Me_2SO-d_6.

The exchange experiments reported in this paper deal with the amide protons being replaced by deuterons. For these experiments commercial Me_2SO-d_6 was stored over CaD_2 (Aldrich Chemical Co.; 99% isotopic purity) overnight under

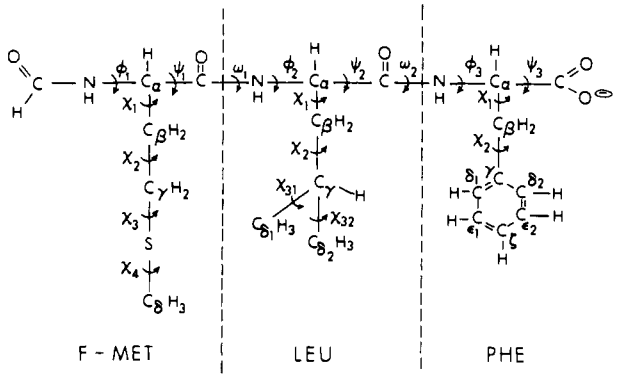

FIGURE 1: Primary sequence of amino acids in FMLP showing the nomenclature used for the three residues (IUPAC–IUB Commission, 1970).

a nitrogen atmosphere and then vacuum distilled from CaD_2 at 2-mm N_2 through previously oven-dried glassware. Only the middle 60% fraction, boiling at 31 °C, was taken. This was then sealed in Teflon plugged septum vials under N_2 (the vials had been previously equilibrated with D_2O vapor in a vacuum desiccator and then baked in a 115 °C oven exposed to the atmosphere). The exchange was performed by dissolving the peptide in D_2O adjusted to the same apparent pH (corrected for pD effect) as the unexchanged samples, using small amounts of DCl and NaOD. The sample was then lyophilized and dried over P_2O_5 in a vacuum oven overnight at 50–60 °C. This was then dissolved in the dried Me_2SO-d_6 and sealed with a pressure cap. This Me_2SO-d_6 was not subjected to freeze–thaw cycles since it had been distilled in a N_2 atmosphere at reduced pressure. All glassware was dried, stored in a desiccator over D_2O, and baked in the oven before use. The work, including the drying of the peptide (after exchange) in the vacuum oven, was done in a N_2 box. The resulting peptide was 92 ± 10% exchanged, and the ^1H spectrum showed no sign of HDO.

NMR Techniques

General. Our 100-MHz (^1H) and 25.15-MHz (^{13}C) NMR apparatus has been described previously (Bleich et al., 1976). We have added a quadrature detection system built in our laboratory (unpublished experiments), and it has also been modified to allow decoupling of deuterons while in the deuteron lock mode (unpublished experiments). The sample temperature was kept to a calibrated value of 30 ± 1 °C via the JEOL temperature controller for both ^{13}C and ^1H experiments. Spin–lattice relaxation was measured by using the standard 180° – τ – 90° – t pulse sequence, with the phase of the 90° pulse changed by 180° on every scan (Cutnell et al., 1976). The 270-MHz (^1H) spectra and relaxation times were obtained on the Bruker spectrometer which forms the "Boston Area High Frequency NMR Research Resource".

Spin–lattice relaxation (T_1) data were processed by using a generalized nonlinear least-squares fitting to

$$(1 - M_Z(t)/M_\infty)/2 = Ce^{-t/T_1} \quad (1)$$

where $M_Z(t)$ is the Z component of nuclear magnetism at time t and M_∞ is the "infinite" time recovery magnetization. The constants C and $1/T_1$ are determined from the raw data.

Computer Methods

All the computer programs described here were written in Fortran IV and executed in double precision on a stand-alone 28K, 16 bit, Texas Instruments Model 980A minicomputer equipped with a 1.15 megaword disc, a Tektronix 4010 nonrefreshed graphics terminal, and a 30-cps printing terminal.

[1] Abbreviations used: FMLP, formyl-L-methionyl-L-leucyl-L-phenylalanine; Me_2SO-d_6, dimethyl-d_6 sulfoxide.

(*1*) *Molecular Modeling Program.* In order to more completely analyze our results we have developed three computer programs of general utility in dealing with peptide conformations. We have given the first program the acronym "PEPTID". This program allows us to store atomic coordinates and dimensions of a large peptide.

The resulting molecule may be conformationally manipulated by specifying the ϕ_i, ψ_i, χ_i and ω_i angles of any residue (the program uses the IUPAC conventions for these angles). The program keeps track of hard-sphere van der Waals contacts. For a given sterically allowed conformation, the distances between any two nuclei may be selectively determined along with the direction cosines of the internuclear vector in the inertial principal axis system. The three moments of inertia in this system are also determined.

Conformations may be displayed on the graphics interface in a variety of model forms. All of the models can be displayed as stereo diimages which may be viewed as three dimensional either by a trained eye directly or with the familiar hand stereo viewers used by many crystallographers. Finally, global and internal rotations in three dimensions for all displays are possible.

The following structural features of FMLP are relevant to the use of PEPTID in this work.

N-Formylmethionyl Residue. The X-ray crystal structure of *N*-formyl-L-methionine has been determined (Chen & Parthasarathy, 1977). They find the *N*-acyl group is in the trans-planar conformation (trans in this nomenclature referring to the oxygen–amide proton conformation). Deviation from planarity is −0.9°. The dimensions and angles relating to the *N*-acyl group available from their study are

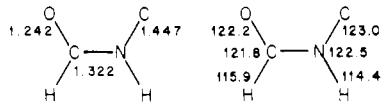

and these were used in program PEPTID.

Peptide Units. We have used the following commonly accepted dimensions for the trans-*planar* ($\omega = 0$) peptide unit (Koetzle et al., 1972) in program PEPTID:

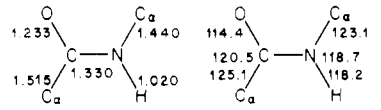

Amide N–H and Side-Chain C–H Distances. The N–H bond length in the dipeptide glycylglycine hydrochloride has been obtained from neutron diffraction (Koetzle et al., 1972). However, in this case the proton was involved in intermolecular hydrogen bonds. In analogy to O–H---O hydrogen bonds where the O–H distances increase with the strength of the hydrogen bond, a similar effect is expected for N–H---O hydrogen bonds of the sort found in peptides. Detailed study of neutron diffraction results which we have performed from available data on a large number of nonpeptide N–H---O hydrogen bonds shows that the effect is smaller in N–H---O bonds than in O–H---O bonds for the same acceptor–donor distances. An extrapolation of the experimental data to infinite acceptor–donor distances gives an unperturbed N–H bond length as 1.020 Å. This is equal to the equilibrium N–H distance resulting from theoretical studies on nitrogen–oxygen–hydrogen bond potential functions (Schroeder & Lippincott, 1957; Chidambaram et al., 1970), and, hence, we have used this value in program PEPTID.

For other bond lengths involving protons attached to carbon, we have used the neutron diffraction values pertaining to either tetrahedral or aromatic carbons as the case applies.

(*2*) *Anisotropic Rotational Diffusion Program.* The second program, given the acronym "WOBBLE", allows us to investigate the rotational dynamics of peptides in solution given experimental input in the form of $^{13}C_\alpha$ relaxation times and direction cosines of the $^{13}C_\alpha$–H vectors with respect to the *diffusional* principal axis system. This program is a minicomputer adaptation of a published work (Berger et al., 1975) but corrects a mathematical oversight in that work.

Given three or more $^{13}C_\alpha$ dipolar T_1's and the direction cosines of the dipolar interaction vector, WOBBLE, using Simplex optimization and the Woessner equations (Woessner, 1962), produces the set of rotational diffusion coefficients, R_i, along the three inertial principal axes which minimizes

$$\chi^2 = \sum_{i\leq 3}\left[\frac{1}{T_{1,\text{exptl},i}} - \frac{1}{T_{1,\text{theory},i}}(R_1,R_2,R_3,l_i,m_i,n_i)\right]^2 \quad (2)$$

where the sum is over the number of vectors and the l_i, m_i, and n_i are direction cosines for each vector. The directional cosines for the $^{13}C_\alpha$–H dipolar interaction vectors are obtained from program PEPTID for a given conformation and used as input parameters for program WOBBLE. A detailed discussion of this procedure and its implications concerning the rotational motion of peptides in solution is presented in a companion paper to this one (Bleich et al., 1979). We discuss there the implications inherent in the assumption made here that inertial and diffusional axial systems are congruent. Since the derivation of rotational diffusion coefficients from ^{13}C–H_α relaxation times depends upon the accuracy with which the internuclear distance is known, a complete discussion of this point is contained in Bleich et al. (1979). For the purposes of the present work, a summary of this is that the C–H_α distance is 1.096 ± 0.01 Å as derived experimentally from a large number of neutron diffraction studies corrected for thermal motion.

(*3*) *Dipolar Relaxation Program.* Given an optimized set R_1, R_2, and R_3 for a given conformation (as determined by program WOBBLE), we have written a simple program called "WOESS" as an obvious extension of the above. For an input internuclear separation and direction cosines, the dipolar relaxation contribution to any ^1H–^1H, ^{13}C–^1H, or ^{14}N–^1H pair can be determined based upon solution of the full Woessner equations.

Results

^{13}C Chemical Shifts. The ^{13}C spectrum of FMLP is shown in Figure 2. ^1H noise decoupling was used with a noise bandwidth of 2.5 kHz. The assignments associated with Figure 2 are given in Table I. The α and β resonances were assigned by using selective heteronuclear spin decoupling and known proton assignments (see ^1H Chemical Shifts and Coupling Constants) as were Met γ and Leu γ. Decoupling of the Leu β and Phe β was done with the solvent peaks inverted by a $180° - \tau - 90°$ pulse sequence with $\tau = 0.4$ s. The Leu β and the Phe β chemical shifts were also checked by using on-resonance deuteron decoupling, with the deuteron irradiation gated on for 0.9 s during accumulation (the deuterium lock was off during this time) and off (deuterium lock on) the remaining time. A pulse repetition of 3 s was used. Figure 2b shows a typical spectrum, with the Me_2SO-d_6 multiplet reduced to one main peak by a suitable choice of the deuterium radio-frequency amplitude.

The chemical shifts for the Phe γ, δ, ϵ, and ζ are based on the assignments for free amino acids and other peptides (Bleich et al., 1977). The δ resonances are straightforward, although we do not distinguish between Leu δ_1 and Leu δ_2.

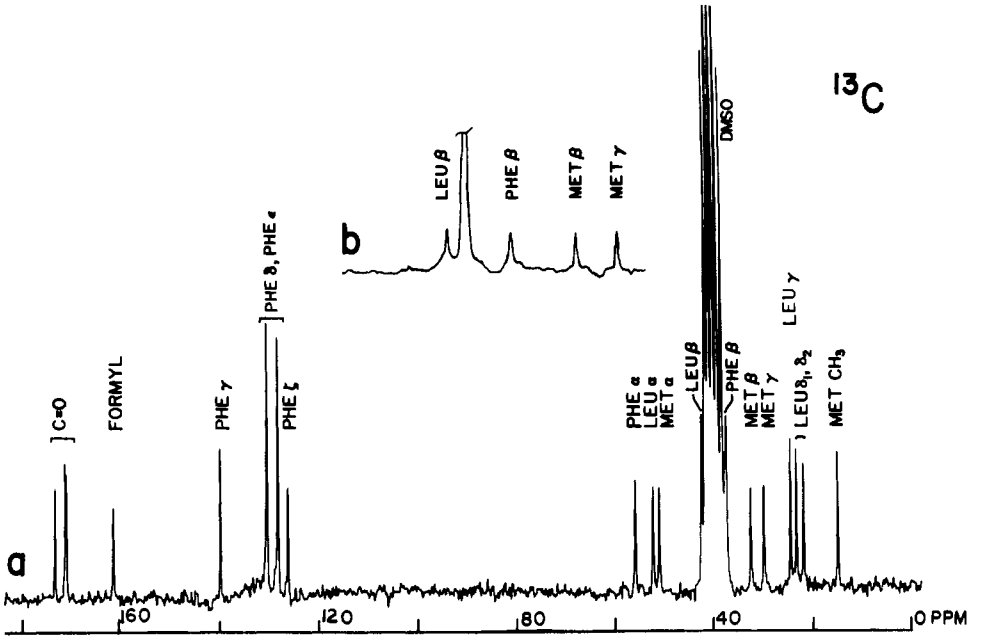

FIGURE 2: (a) The 25.15-MHz ^{13}C spectrum of FMLP at 30 °C and 0.05 M in Me_2SO-d_6 (bandwidth = 5.0 kHz; number of transients = 12000; 90° pulse repetition = 12.0 s; pulse width = 22 μs; number of data points = 8192). Chemical shifts are measured downfield with respect to external tetramethylsilane (Me_4Si), whose resonance location was established by using a separate sample containing a solution of Me_4Si in Me_2SO-d_6. (b) Spectrum taken by using on-resonance deuterium decoupling showing detail of the resonances normally under the solvent envelope (see text).

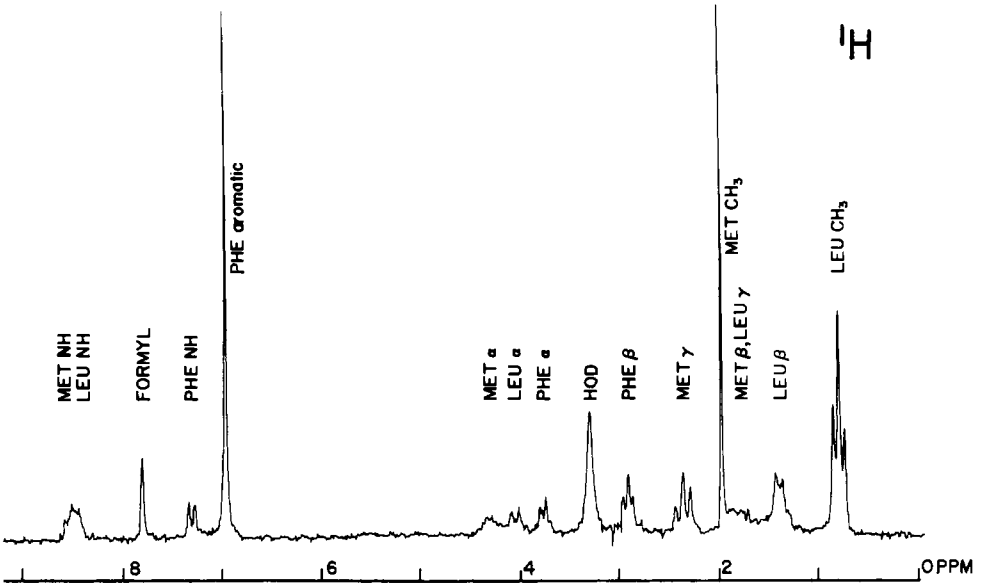

FIGURE 3: The 100.0-MHz ^1H spectrum of FMLP at 30 °C and 0.05 M in Me_2SO-d_6 (bandwidth = 1.0 kHz; number of transients = 10; 90° pulse repetition = 10 s; pulse width = 18.2 μs; number of data points = 8192). Chemical shifts are measured downfield with respect to external tetramethylsilane (as described in the caption to Figure 2a).

We did not attempt a complete assignment of the carbonyl resonances and only note that the peak at δ = 170.6 is due to the Phe carbonyl as determined by comparison to a spectrum taken at low pH.

The possibility of intermolecular interactions was probed by measuring the chemical shifts at 0.03, 0.01, and 0.005 M after accumulating 10000, 68000, and 250000 transients, respectively. 1,4-Dioxane was present in each sample as a reference. The chemical shift with respect to 1,4-dioxane of each resonance was the same, to ±0.1 ppm, for each concentration.

^1H Chemical Shifts and Coupling Constants. The 100-MHz ^1H spectrum of FMLP is shown in Figure 3, and associated data at 100 and 270 MHz are given in Tables II and III. In the assignment of the amide resonances, we were aided by using homonuclear spin decoupling of the α-^1H resonances. The latter were assigned by decoupling of the β protons.

The temperature dependences of the amide chemical shifts are given in Table IV for pH 8 and low pH (~5; the sample was prepared by direct dissolution in Me_2SO-d_6 with no adjustments). The slopes were obtained by using linear regression.

^1H and ^{13}C Relaxation Times. All T_1's given reflect the result of using data from several different runs. A typical superimposed data plot, in this case for the ^{13}C-labeled Leu α, is given in Figure 4. The repetition rate was usually 5 times the value of the measured T_1 with the exception of the ^{13}C-labeled carbonyl (repetition ~3.7 times the longest relaxation). A single ^{13}C datum was usually the result of a 1-h accumulation time. We required at least three consistent "T_∞"

Table I: ^{13}C NMR Parameters for F-Met-Leu-Phe-O$^-$ in Me_2SO-d_6, at 25 MHz and 30 °C

resonance	δ	T_1 (s)	intercept	NOE
formyl CH	160.9 ± 0.1	0.256 ± 0.026	0.91	2.4
methionyl				
α	50.5 ± 0.1	0.221 ± 0.014	0.97	2.9
β	32.2 ± 0.1	0.183 ± 0.012	0.91	2.8
γ	29.5 ± 0.1	0.290 ± 0.028	0.90	2.6
δ	14.6 ± 0.1	2.53 ± 0.22	0.90	2.7
leucyl				
α	51.7 ± 0.1	0.194 ± 0.009	0.96	2.5
β	40.8[a] ± 0.1	0.184 ± 0.015[a]	0.90	
γ	24.1 ± 0.1	0.354 ± 0.012	0.90	2.8
δ_1	22.9 ± 0.1	0.542 ± 0.060	0.90	2.9
δ_2	21.5 ± 0.1	0.557 ± 0.060	0.90	2.9
phenylalanyl				
α	55.3 ± 0.1	0.195 ± 0.012	1.02	2.5
β	37.2[a] ± 0.2	0.161 ± 0.018[a]	0.88	
γ	139.1 ± 0.1	2.86 ± 0.24	1.01	2.4
δ_1, δ_2	129.6 ± 0.1	0.400 ± 0.012	0.99	2.9
ϵ_1, ϵ_2	127.4 ± 0.1	0.413 ± 0.041	0.96	2.8
ζ	125.4 ± 0.1	0.275 ± 0.020	0.96	2.9
carbonyls				
	172.5	4.33 ± 0.60	0.97	2.2
(Phe)	170.6	2.80 ± 0.45	0.97	2.2
	170.4	2.60 ± 0.10	0.98	2.2

[a] Overlapped by Me_2SO-d_6; T_1's measured during gated deuteron decoupling.

values obtained at the beginning, middle, and end of each experiment.

The ^{13}C T_1's determined for each resonance of FMLP are given in Table I. All resonances are characterized by a single T_1. We did not accept any data with an intercept outside of 1.0 ± 0.1. Due to the overlapping of the Me_2SO-d_6 multiplet (Figure 2a), the relaxation of the Leu β and the Phe β could only be measured from the τ values when the Me_2SO-d_6 peaks were still inverted, but the Leu β and the Phe β resonances recovered through the null; the resulting intercepts of the T_1 plots were approximately 0.8. The relaxation of the Leu β and the Phe β was thus measured in the presence of gated deuteron decoupling, described in the previous section.

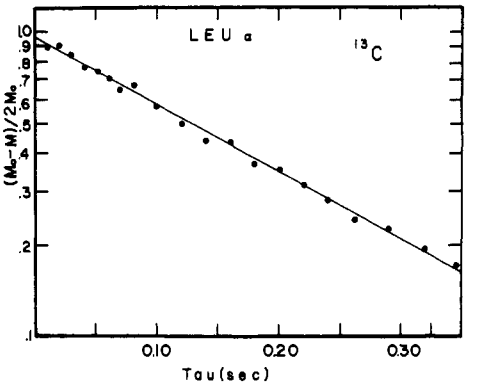

FIGURE 4: A typical semilogarithmic data plot for the ^{13}C-labeled Leu α. Measurements were taken using a $(180° - \tau - 90°-)_n$ pulse sequence at 25.15 MHz.

The ^1H T_1's are given in Table II and Table III for 100 and 270 MHz, respectively. None of the resonances whose ^1H relaxation behavior is analyzed here, i.e., α, formyl, and amide protons, are part of a tightly coupled spin system. Hence, the nonselective excitation methods used here are entirely adequate. All resonances for normal and 91% exchanged material are described by a single T_1. As evidence for the accuracy of our experimental relaxation times *and* our method of treating the raw data by nonlinear regression, we have also included in Table II relaxation times derived for the completely exchanged form on the basis of experimental data obtained for 60% exchanged peptide. Thus, in this case we fit the data via the regression program to

$$\frac{1 - M_Z(t)/K}{2} = C[0.4e^{-\tau/T_{1,\text{normal}}} + 0.6e^{-\tau/T_{1,\text{other}}}] \quad (3)$$

where we assume $T_{1,\text{normal}}$ to be known and identical with the unexchanged material. The program solves for C and $T_{1,\text{other}}$. Clearly, the data sets agree very well.

As expected for a molecule of this size, heteronuclear Overhauser enhancements, performed as previously described (Bleich et al., 1976), indicate that only dipole–dipole interactions contribute to ^{13}C–H_α relaxation. We have assumed this to be true for all ^1H relaxation times discussed here.

Table II: ^1H NMR Spectral Parameters for Normal and Exchanged FMLP in Me_2SO-d_6 at 100 MHz and 30 °C[a]

resonance	δ	$T_{1,\text{normal}}$ (s)	intercept normal	$T_{1,\text{exch}}$ (s)	intercept exch
formyl	7.98 ± 0.01	0.827 ± 0.030	0.99	2.551 ± 0.130 (2.99 ± 0.02)	0.98
methionyl					
amide	8.79 ± 0.01	0.248 ± 0.016	0.95		
α	4.40 ± 0.01	0.376 ± 0.031	0.96	0.664 ± 0.031 (0.670 ± 0.02)	0.99
β_1	1.98 ± 0.04	0.280[b]	0.99	0.280 ± 0.020 (0.252 ± 0.025)	1.02
β_2	1.80 ± 0.04				
γ	2.42 ± 0.01	0.290 ± 0.008	1.00	0.357 ± 0.017 (0.325 ± 0.011)	0.97
δ	2.03 ± 0.01	1.33 ± 0.05	1.01	1.45 ± 0.06 (1.30 ± 0.10)	0.94
leucyl					
amide	8.72 ± 0.01	0.174 ± 0.012	0.97		
α	4.15 ± 0.01	0.367 ± 0.028	0.97	0.534 ± 0.022 (0.535 ± 0.035)	0.98
β_1	1.45 ± 0.05	0.200 ± 0.013	0.98	0.195 ± 0.005 (0.231 ± 0.008)	1.00
β_2					
γ	1.57 ± 0.03	0.280[b]	0.91	0.223 ± 0.014	1.00
δ_1	0.86 ± 0.01	0.321 ± 0.010	0.99	0.324 ± 0.011 (0.330 ± 0.337)	0.99
δ_2	0.77 ± 0.01				
phenylalanyl					
amide	7.48 ± 0.01	0.210 ± 0.016	1.03		
α	3.82 ± 0.01	0.573 ± 0.041	0.96	0.700 ± 0.030 (0.661 ± 0.034)	1.00
β_1	3.04 ± 0.01	0.153 ± 0.010	0.99	0.140 ± 0.007 (0.177 ± 0.024)	1.00
β_2	2.92 ± 0.01				
aromatic	7.1 ± 0.05	0.808 ± 0.074	1.02	0.804 ± 0.041 (0.792 ± 0.027)	1.02

[a] Parenthetical values are derived from 60% exchanged material via a two-parameter fit of experimental data (see text). [b] Overlapping resonances.

Table III: ^{1}H NMR Spin-Lattice Relaxation Times for Normal and Exchanged FMLP in Me_2SO-d_6, at 30 °C and 270 MHz

resonance	$T_{1,\text{normal}}$ (s)	intercept normal	$T_{1,\text{exch}}$ (s)	intercept exch
formyl	1.368 ± 0.077	0.88	3.63 ± 0.16	0.89
methionyl				
amide	0.400 ± 0.021	0.87		
α	0.595 ± 0.017	0.88	0.920 ± 0.032	0.88
β_1	0.449 ± 0.042	0.72	0.292 ± 0.036	0.88
β_2	0.340 ± 0.020	0.81	0.243 ± 0.020	1.00
γ	0.368 ± 0.006	0.89	0.462 ± 0.022	0.81
δ	1.543 ± 0.038	0.92	1.54 ± 0.18	0.90
leucyl				
amide	0.288 ± 0.011	0.85		
α	0.596 ± 0.015	0.88	0.748 ± 0.025	0.93
β_1	0.243 ± 0.003	0.89	0.266 ± 0.023	0.83
β_2	0.235 ± 0.012	0.85	0.204 ± 0.018	0.94
γ	0.496 ± 0.020	0.90	0.572 ± 0.036	0.92
δ_1	0.377 ± 0.007	0.92	0.370 ± 0.020	0.89
δ_2	0.391 ± 0.008	0.91	0.373 ± 0.015	0.91
phenylalanyl				
amide	0.357 ± 0.012	0.89		
α	0.820 ± 0.023	0.90	1.008 ± 0.016	0.86
β_1	0.277 ± 0.013	0.89	0.258 ± 0.025	0.81
β_2	0.273 ± 0.026	0.88	0.233 ± 0.013	0.92
aromatic	1.175 ± 0.033	0.88	1.14 ± 0.05	0.91

Table IV: Chemical Shift vs. Temperature from Amide Proton Data for FMLP at 100 MHz (0.05 m; Me_2SO-d_6)

	chemical shift vs. temp (× 10^{-3} ppm/deg)		coupling constant (Hz)	
residue	low pH	pH 8	low pH	pH 8
Met	4.1 ± 0.2	8.5 ± 0.5	8.3 ± 0.3	8.5 ± 0.5
Leu	4.5 ± 0.2	8.5 ± 0.5	8.3	8.4 ± 0.5
Phe	6.1 ± 0.2	2.6 ± 0.3	8.3	6.6 ± 0.3

Proton Spin–Spin Coupling Constants. The observed and derived ^{1}H spin–spin coupling constants for FMLP are given in Table V. All were measured from 270-MHz spectra taken at 30 °C.

Each amide doublet is well resolved, and the coupling constants were observed directly.

The Met α–β coupling constant was derived by using homonuclear spin decoupling applied at the γ resonance. The resulting Met β resonance is a nonoverlapping doublet, each containing four peaks. The coupling constants were derived from the appropriate second-order equations after considering the AB part of an ABX spin system (Pople et al., 1959). The predicted chemical shifts and intensities agree satisfactorily with the measured Met β_1 and β_2 chemical shifts and intensities (Figure 5).

The Leu α–β spin system analysis could not be aided by direct homonuclear decoupling, since the γ resonance is too close to the β resonance. We thus proceeded as follows. By decoupling at Leu α, we determined what peaks of the Leu β are due to Leu γ (the peak that does not coalesce; see Figure 5a). The remaining peaks were then assumed to be overlapping doublets due to the nonchemical-shifted β's (Figure 5b), an argument which is supported by the Leu α resonance structure in the exchanged sample. The coupling constants thus obtained, while approximate, agree well with the average values of Leu α–β coupling constants given in other published reports (Cowburn et al., 1977; Fischman et al., 1978).

The Leu γ–δ_1 and γ–δ_2 coupling constants were directly observed from the corresponding doublet.

The Phe α–β coupling constant is easily derived from the β portion of the spectrum, where a well-defined octet is observed. As in the Met case, we use the ABX analysis directly. The predicted chemical shifts and intensities agree with those observed (Figure 5).

Table V: Observed and Derived ^{1}H Spin–Spin Coupling Constants for FMLP in Me_2SO-d_6, 30 °C, from 270-MHz Spectra[a]

resonance	spin system and constants[b]		
formyl		$^3J_{CHNH} = 0.0$	
methionyl			
amide		$^3J_{NHCH} = 8.5 \pm 0.5$	
α–β	$\delta_A = 1.98$	$\lvert J_{AB}\rvert = 14.8$	
	$\delta_B = 1.80$		
	$\delta_X = 4.40$	$J_{AX} = 4.4$	$P_I = 0.65 \pm 0.03$
			$P_{II} = 0.08 \pm 0.04$
		$J_{BX} = 9.1$	$P_{III} = 0.27 \pm 0.02$
leucyl			
amide		$^3J_{NHCH} = 8.4 \pm 0.5$	
α–β	$\delta_A = 1.46$	$\lvert J_{AB}\rvert = 14.0$	
	$\delta_B = 1.46$		
	$\delta_C = 4.15$	$J_{AX} = 7.5$	$P_I = 0.54 \pm 0.04$
			$P_{II} = 0.45 \pm 0.05$
		$J_{BX} = 7.5$	$P_{III} = 0.01 \pm 0.03$
γ–δ	$\delta_A = 1.57$	$J_{AX_1} = 6.7$	
	$\delta_{X_1} = 0.86$		
	$\delta_{X_2} = 0.77$	$J_{AX_2} = 6.2$	
phenylalanyl			
amide		$^3J_{NHCH} = 6.6 \pm 0.3$	
α–β	$\delta_A = 3.04$	$J_{AB} = 12.9$	$P_I = 0.12 \pm 0.03$
	$\delta_B = 2.92$		$P_{II} = 0.35 \pm 0.04$
	$\delta_X = 3.82$	$J_{AX} = 6.1$	$P_{III} = 0.54 \pm 0.02$
		$J_{BX} = 4.7$	

[a] For classical rotamers: P_I, $\chi_1 = -60°$; P_{II}, $\chi_1 = +180°$; P_{III}, $\chi_1 = +60°$. Convention: $\delta_A > \delta_B$. [b] J values are in units of hertz.

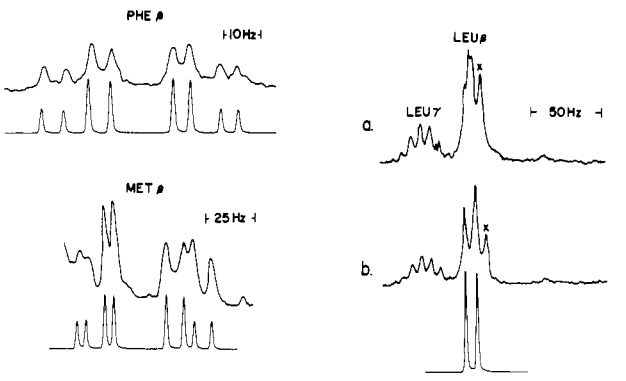

FIGURE 5: The 270-MHz observed and predicted β-proton spin multiplets for the ionized form of FMLP in Me_2SO-d_6. (a) Leucine β as observed and (b) with α protons decoupled. (×) Indicates nonspin coupled interfering resonance.

φ Values from $^3J_{NHCH}$ Coupling Constants. In the study of the conformation of peptides, it is usually assumed that the coupling constant $^3J_{NHCH}$ is related to the dihedral angle φ by a function of the form (Karplus, 1963)

$$J = A \cos 2\theta - B \cos \theta + C \qquad (4)$$

where A, B, and $C > 0$ and $\theta = |\phi - 60°|$. From semiempirical studies many authors have expressed J using a similar function. In Table VI (a) we summarize several of these relations in a standard form for purposes of comparison.

For this work we prepared a plot of J vs. φ superimposing all of the eight relations given in Table VI (a). For a measured value of $^3J_{NHCH}$, we corrected the electronegativity effects (Bystrov et al., 1978) as

$$J_{cor} = 1.09 J_{obsd} \qquad (5)$$

The figure was used to determine the uncertainty in the al-

Table VI

(a) J_{NHCH} vs. θ for Trans Peptide	ref
$J_1 = 11.27\cos^2\theta - 4.32\cos\theta + 0.01$	Barfield & Gearhart (1973)
$J_2 = (8.0 + 0.9)\cos^2\theta - (0.9 \pm 0.9)\cos\theta + 0.9 \pm 0.9$	Bystrov et al. (1969)
$J_3 = 9.56\cos^2\theta - 0.42\cos\theta + 0.12$	Schwyzer (personal communication)[a]
$J_4 = 9.0\cos^2\theta - 3.3\cos\theta - 0.3$	Thong et al. (1969)
$J_5 = 9.2\cos^2\theta - 1.5\cos\theta - 1.3$	Ramachandran et al. (1971)
$J_6 = 9.4\cos^2\theta - 1.1\cos\theta + 0.4$	Bystrov et al. (1973)
$J_7 = 7.11\cos^2\theta - 2.33\cos\theta + 1.51$	Mitra (1978)
$J_8 = 8.6\cos^2\theta - 2.9\cos\theta + 0.0$	Cung et al. (1974)

(b) Range of ϕ Values from Modified Karplus Equations		
ϕ_1 (deg)	ϕ_2 (deg)	ϕ_3 (deg)
−80 to −110	−80 to −110	−70 to −90; +60 to +80
−130 to −160	−130 to −160	−150 to −170; +40 to +60

(c) $^3J_{NHCH_\alpha}$ Coupling Constants in Chemotactic Peptide Fragments (Me_2SO-d_6, 30 °C)

fragment	pH*	coupling constant (Hz)
F-Met	2	8.6
F-Leu	2	8.4
F-Met-Phe	2	8.4 (Met)
		8.6 (Phe)
F-Met-Phe	8	8.3 (Met)
		6.4 (Phe)
Met-Leu-Phe	2	8.3 (Leu)
		7.6 (Phe)
Met-Leu-Phe	8	8.6 (Leu)
		6.4 (Phe)
F-Met-Leu-Phe	2	8.5 (Met)
		8.1 (Leu)
		8.6 (Phe)
F-Met-Leu-Phe	8	8.5 (Met)
		8.4 (Leu)
		6.6 (Phe)

[a] Schwyzer, personal communication in Weinkam & Jorgensen (1971).

lowed ϕ values. That is, for a given corrected J we assumed that, because the functional relation between J and ϕ is not known uniquely, the ϕ value may lie anywhere within the limits of the most extreme predictions of ϕ for a given J_{cor}. These allowed values are given in Table VI (b).

During the course of these experiments we determined $^3J_{NHCH}$ for several model compounds and observed a hitherto unreported effect. This is the change of C-terminal $^3J_{NHCH}$ coupling constants with pH. Data are given in Table VI (c). It appears that the correction factor given above for electronegativity is not applicable to these C-terminal coupling constants. Thus, the observed constants appear consistently smaller in the protonated carboxylate forms than in the zwitterionic forms by about 2 Hz. We believe that this is not a conformational effect and the result has important implications for the work reported here, as well as future work on open-chain peptides.

Side-Chain Rotamer Populations from Spin Coupling Constants. The derived J_{AX} and J_{BX} coupling constants were analyzed in terms of populations of the three classical rotamers, as shown in Table V, using the equations

$$J_{AX} = 4.1P_I + 11.7P_{II} + 2.9P_{III}$$
$$J_{BX} = 12.0P_I + 2.1P_{II} + 4.7P_{III} \quad (6)$$
$$1 = P_I + P_{II} + P_{III}$$

suggested by Feeney (Feeney, 1976). In Table V and below, the rotamers are defined by $P_I(g^+)$, $\chi^1 = 180°$ and $P_{III}(g^-)$, $\chi^1 = 60°$. For reference in the following discussion, Table VII

Table VII: Comparison between Side-Chain (χ_1) Conformations for FMLP Residues in Solution and Those Found for the Same Residues in a Variety of Proteins and Peptides in the Solid State

residue compd	rotamer populations g^+	t	g^-	ref
methionine				
FMLP	0.65	0.08	0.27	this work
19 proteins	0.52	0.39	0.09	Janin et al. (1978)
10 peptides	0.40	0.30	0.30	Chen & Parasarathy (1977)
leucine				
FMLP	0.54	0.45	0.01	this work
19 proteins	0.60	0.36	0.04	Janin et al. (1978)
22 peptides	0.70	0.30	0.00	Benedetti (1977)
phenylalanine				
FMLP	0.54	0.35	0.12	this work
22 peptides	0.45	0.35	0.20	Benedetti (1977)
17 peptides/ amino acid derivatives	0.12	0.47	0.41	Cody et al. 1973
15 proteins	0.07	0.26	0.67	Chandresekaran & Ramachandran (1970)
theory	0.19	0.36	0.45	Chandresekaran & Ramachandran (1970)

contrasts results obtained in this work with side-chain conformations from published data for the same residues obtained in solids by diffraction techniques. The coupling constant analysis described above is not sensitive to interchange of g^+ and g^-. In order to compare derived populations of rotamers, we have chosen assignments consistent with theory.

(*1*) *Methionine.* Our results indicate that the conformers g^+ and g^- are overwhelmingly favored. Studies of methionine containing peptides in the solid state (Chen & Parthasarathy, 1977) show that χ^2 is highly correlated with χ^1. With $\chi^1 = \pm 60°$, $\chi^2 = \chi^3 = \pm 180°$ is favored on steric grounds. Extensive computer experiments with PEPTID confirm this, and consequently we have assumed the conformation of the formylmethionine side chain to be g^+tt,g^-tt in FMLP.

(*2*) *Leucine.* Our work indicates that the χ^1 conformer g^- is absent. In addition our computer experiments show that χ^2 is correlated with χ^1 insofar as only $\chi^2 = 0°$ is sterically allowed in FMLP. Hence, our assumption is that only the conformers $g^+(0°)$ and $t(0°)$ are populated.

(*3*) *Phenylalanine.* A critical comparison of available experimental and theoretical work on phenylalanyl residues in a variety of compounds (references in Table VI) shows that, whatever the populations of χ^1 rotamers, the χ^2 angle is restricted to the region around 90°. Our computer experiments show this clearly. In fact only the choice $\chi^2 = 85°$ allows all of the χ^1 conformers to be populated in FMLP. Hence, our assumption is that this residue's rotamers are $g^+(85°),t(85°),g^-(85°)$.

(*4*) *General.* In this work the simplifying assumption has been made that the lifetimes of rotameric states are comparable to, or longer than, molecular reorientation times. This allows us to deduce, using the conclusions just discussed, that there is a distribution of 27 different molecules (3 side chains, each with 3 possible χ^1 conformers arranged randomly) at any given time. The normalized weights of these are given in Table VIII on the basis of the observed rotamer populations. Table VIII also lists the side-chain angles corresponding to each alphabetically designated element. Of these 27 possible molecules, C, D, E, F, I, M, MM, N, U, V, and W add up to a weight of 1% of the total. Molecules J, K, O, P, R, S, T, X, Y, and Z, on the other hand, comprise 90% of the total. In the calculations below this latter value has been renormalized to 100% and assumed to be the total set.

Table VIII

(a) χ^1 Torsional Angle Matrix Used in Program PEPTID

χ^1 residue:	A	B	C	D	E	F	G	H	I
label: Met	180°	180°	180°	180°	180°	180°	180°	180°	180°
Leu	180°	180°	180°	60°	60°	60°	−60°	−60°	−60°
Phe	180°	60°	−60°	180°	60°	−60°	180°	60°	−60°
χ^1 residue:	J	K	L	M	MM	N	O	P	Q
label: Met	60°	60°	60°	60°	60°	60°	60°	60°	60°
Leu	180°	180°	180°	60°	60°	60°	−60°	−60°	−60°
Phe	180°	60°	−60°	180°	60°	−60°	180°	60°	−60°
χ^1 residue:	R	S	T	U	V	W	X	Y	Z
label: Met	−60°	−60°	−60°	−60°	−60°	−60°	−60°	−60°	−60°
Leu	180°	180°	180°	60°	60°	60°	−60°	−60°	−60°
Phe	180°	60°	−60°	180°	60°	−60°	180°	60°	−60°

(b) Derived Fractional Statistical Weights, f_i, for Conformers Listed in Table VI (a)

	A	B	C	D	E	F	G	H	I
f_i:	0.013	0.019	0.004	0.0003	0.0004	0.0001	0.015	0.023	0.005
	J	K	L	M	MM	N	O	P	Q
f_i:	0.039	0.061	0.0135	0.001	0.0014	0.0003	0.047	0.073	0.016
	R	S	T	U	V	W	X	Y	Z
f_i:	0.106	0.163	0.036	0.002	0.004	0.001	0.127	0.195	0.043

$$\sum_i f_i = 1.009$$

Rotational Diffusion Coefficients for FMLP. Our results (Table I) show that the four observed ^{13}CH, main chain, relaxation times are almost identical. However, detailed analysis, using program WOBBLE (Bleich et al., 1979), shows that, in fact, rotational diffusion is highly anisotropic for all sterically allowable conformations. Thus, identical values of $^{13}C-H_\alpha$ relaxation times in peptides *cannot* be taken to indicate isotropic reorientation able to be characterized by a single reorientation time. For example, for the family of side-chain rotamers (above) superimposed on our proposed main-chain conformation, the average diffusion coefficient $\langle R \rangle \simeq 0.1 \times 10^{10}\ s^{-1} = {}^1/_3(R_1 + R_2 + R_3)$ varies by about 30% over the range of conformations while the anisotropy factor $\Delta R = (R_1^2 + R_2^2 + R_3^2 - R_1R_2 - R_1R_3 - R_2R_3)^{1/2}$ varies by about 120%.

The relaxation times predicted in this paper are on the basis of rotational reorientation times derived for each rotamer main-chain permutation by using PEPTID to give inertial system coordinates and WOBBLE plus observed $^{13}C-H_\alpha$ T_1's to derive the rotational diffusion coefficients.

Discussion

General. The purpose of this work is to determine a set of intramolecular, noncovalent, proton–proton distances in peptide molecules in solution.

Several recent papers have emphasized the use of proton spin–lattice relaxation times (Hayashi et al., 1977; Bleich et al., 1976) or nuclear Overhauser enhancements (Khaled & Urry, 1976; Glickson et al., 1976; Leach et al., 1977) to aid in the determination of peptide conformations in solution. The basic problem is determining proton spectral density functions $J(h\omega_i)$. It makes little difference if these appear as an appropriate sum (for relaxation methods) or a corresponding division of sums (for Overhauser methods) in the equations relating the observable (T_1 or NOE) to the desired internuclear distances between dipole–dipole paired protons. For this reason we will refer to the methods as spectral density function methods (SDFM) in the following analysis.

We have used nonselective pulse methods in this work because we are not analyzing relaxation in closely coupled spin systems (where cross relaxation might be important). We have no evidence for cross correlation effects in any of our relaxation measurements. Spin-diffusion mechanisms are not effective in peptides of this size.

Assuming individual structures under investigation to be rigid on the rotational diffusional time scale, all SDFM require the characterization of the angular diffusional motion of each structure. We have given our approach to the solution of this part of the problem briefly above and in detail (Bleich et al., 1979). We have shown by direct calculation on the peptide under study that $^{13}C-H_\alpha$ relaxation times which are extremely close to one another may correspond to widely different sets of rotational diffusion rates. As a minimal requirement, any study of conformation by SDFM must therefore examine the iso-/aniso-tropic diffusion models carefully for the particular molecule involved.

After we solve for ^{13}C spectral densities, SDFM then requires the transfer of the parameters involved to yield proton spectral densities. This is easily done, but the application of the resulting equations involves the realization that frequency dependence of the spectral densities (themselves complicated by the anisotropic reorientation of the molecule) is more important for protons than for ^{13}C at all presently obtainable observation frequencies. Thus, we show below that even for the tripeptide under study the ^{1}H spectral densities must be frequency corrected at 100 MHz.

After having derived the requisite proton spectral densities, the SDFM diverge, as mentioned above, only in the manner in which they are combined with proton T_1 or NOE measurements. We believe that relaxation times determined, as they are, from multipoint data sets are inherently more accurate than NOE's determined from area ratios (although the former is much more time consuming). For this reason we confine our discussion and experimental data to the relaxation branch of SDFM.

We have chosen this particular tripeptide as an exposition of the problems facing SDFM because the observed $^3J_{NHCH}$ coupling constants indicate that the molecule has essential rigidity in its backbone (see below). The molecule is also simple enough to allow conformational conclusions to be drawn which may be seen quite directly. We have discussed the problem of peptide flexibility and methods of attack on the problem in another publication (Bleich & Glasel, 1978). Suffice it to say here that for general, open-chain, nonrigid peptides the study of intramolecular motions will require advances in both theory and experiment before valid detailed conclusions can be anticipated.

Our general procedure, now to be discussed, takes us from the assumption of rigidity to conformational data in a logical succession. Beginning with a range of ϕ angles determined by $^3J_{NHCH}$ coupling constants, we identify a range of ψ values which are allowed on a steric Ramachandran plot. For these conformations we then investigate, using WOBBLE, PEPTID, and ^{13}C α-carbon T_1 data, the three rotational diffusion coefficients associated with each conformation. These are then used to predict proton relaxation times for α protons in the absence of dipolar interactions with the amide protons (the interaction having been removed by exchanging the amide protons with deuterons). Conversely, we require the observed amide proton relaxation times, taking into account ^1H–^1H and ^1H–^{14}N contributions, to agree with the structural predictions. These data are used to confirm the ϕ angle and to determine the contributions from other protons in the system. The fit is made to experimental data taken at 100 and 270 MHz. This procedure is continued until an acceptable fit of prediction to experiment is obtained for major contributing dipole–dipole interactions to α and amide proton relaxation.

Proton Spin–Lattice Relaxation. The following discussion gives our mathematical procedure for the transfer of molecular spectral density information (derived from ^{13}C–H_α data) into intramolecular proton–proton distances with the aid of measured proton spin–lattice relaxation times.

For a rigid molecule of arbitrary shape, spectral density functions in the absence of cross-correlation effects, and in the axis system where the diffusion tensor is diagonal with direction cosines l, m, and n with respect to the principal axes, are given by the Woessner equations (Woessner, 1962) transformed here to eliminate a singularity. The spectral density functions are

$$J(\omega_i) = \frac{12Rd(\omega_i^2 + 36L^2)}{(1/\tau_+^2 + \omega_i^2)(1/\tau_-^2 + \omega_i^2)} - \frac{12e(\omega_i - 36L^2)}{(1/\tau_+^2 + \omega_i^2)(1/\tau_-^2 + \omega_i^2)} + \frac{C_1\tau_1}{(1 + \omega_i^2\tau_1^2)} \frac{C_2\tau_2}{(1 + \omega_i^2\tau_2^2)} + \frac{C_3\tau_3}{(1 + \omega_i^2\tau_3^2)} \quad (7)$$

with

$$R = \frac{1}{3}(R_1 + R_2 + R_3)$$

$$L^2 = \frac{1}{3}(R_1R_2 + R_1R_3 + R_2R_3)$$

$$1/\tau_+ = 6[R + (R^2 - L^2)^{1/2}]$$

$$1/\tau_- = 6[R - (R^2 - L^2)^{1/2}]$$

$$1/\tau_1 = 4R_1 + R_2 + R_3$$

$$1/\tau_2 = 4R_2 + R_1 + R_3$$

$$1/\tau_3 = 4R_3 + R_1 + R_2$$

$$d = \frac{1}{2}[3(l^4 + m^4 + n^4) - 1]$$

$$e = \frac{1}{6}[\delta_1[(3l^4 + 6m^2n^2) - 1] + \delta_2[(3m^4 + 6l^2n^2) - 1] + \delta_3[(3n^4 + 6l^2m^2) - 1]]$$

$$C_1 = 6m^2n^2 \qquad C_2 = 6l^2n^2 \qquad C_3 = 6l^2m^2$$

$$\delta_1 = R_1 - R \qquad \delta_2 = R_2 - R \qquad \delta_3 = R_3 - R$$

in which R_1, R_2, and R_3 are the elements of the diagonalized anisotropic rotational diffusion tensor.

The resulting formula for calculating proton–proton dipolar relaxation rates is

$$\frac{1}{T_1} = \frac{9}{8}\frac{\gamma_H^4\hbar^2}{r_{HH}^6}\left[\frac{2}{15}J(\omega_H) + \frac{8}{15}J(2\omega_H)\right] \quad (8)$$

where r_{HH} is the magnitude of the proton–proton internuclear vector, and γ and $\hbar$ have their usual meaning. The unknowns in our work are, of course, r_{HH}.

For a given proton it is assumed that individual dipolar contributions to overall $1/T_1$ are additive. This sum must be carried out, in a peptide, over all neighboring ^1H and ^{14}N nuclei.

The case for dipolar relaxation of a proton attached to a nucleus, such as ^{14}N, containing an electric quadrupole moment is *not* straightforward for all values of R_i. However, for molecules of molecular weight up to several thousand (specifically excluding proteins), the theory of Kimmich (1977) applies as the "high-field" case when the protons are observed at frequencies of 100 MHz or greater (Bleich et al., 1978) for protons attached to ^{14}N. In this limit

$$1/T_1 = \frac{2}{15}\frac{\gamma_H^2\gamma_N^2\hbar^2}{r_{NH}^6}[J(\omega_H - \omega_N) + 3J(\omega_H) + 6J(\omega_H + \omega_N)] \quad (9)$$

where the spectral density functions are given as shown in eq 7 with the appropriate frequencies substituted.

Detailed Procedure. The logical procedure we use to analyze the raw data is shown, in the form of a flow diagram, in Figure 6. The method of determining the ϕ_i and χ_i^1 angles of the main and side chains has already been described. We use a conventional steric Ramachandran plot (Gibbons et al., 1970) to identify the range of possible values for the ψ_i torsional angle. Of the various torsional angles in FMLP, only the conformation of the angle involving the rotation of the formyl group with respect to the methionyl amide proton is considered absolutely defined as 0°. This is on the basis of the observed zero coupling constant which is in accord with similar observations on model compounds such as *N*-methylformamide and other structures (Robin et al., 1970) and with the solid-state structure of *N*-formylmethionine (Chen & Parathasarathy, 1977). The large values of $^3J_{NHCH}$ for two of the residues of FMLP [much larger than observed in short-chain peptides (Gupta-Bhaya, 1975)] lead us to the assumption that the molecule has rigidity with respect to the $-CH_\alpha$-NH– units on a millisecond or longer time scale. Similar conclusions have recently been arrived at on the same grounds for a dissimilar tetrapeptide (Hallenga & Van Binst, 1979). In our case the only questionable residue in this regard is the C-terminal phenylalanine. Here, we find that the $^3J_{NHCH}$, using normal electronegativity corrections, would indicate possible dynamic averaging. However, as discussed in a previous section, our work with model compounds indicates that the electronegativity correction for the carboxylate form of a C-terminal residue's amide coupling constant is of the order of 2 Hz. This would bring the corrected coupling constant well up into the value where rigidity can be safely assumed.

For each set of main-chain torsion angles within the allowed range, we allow PEPTID to determine whether or not any of the 27 side-chain conformers is sterically disallowed. For any main-chain conformation we require the set of 10 most populated side-chain conformers to be allowed. This van der Waals "trap" is similar to the technique used in determinations of conformations from lanthanide ion perturbation techniques (Barry et al., 1974).

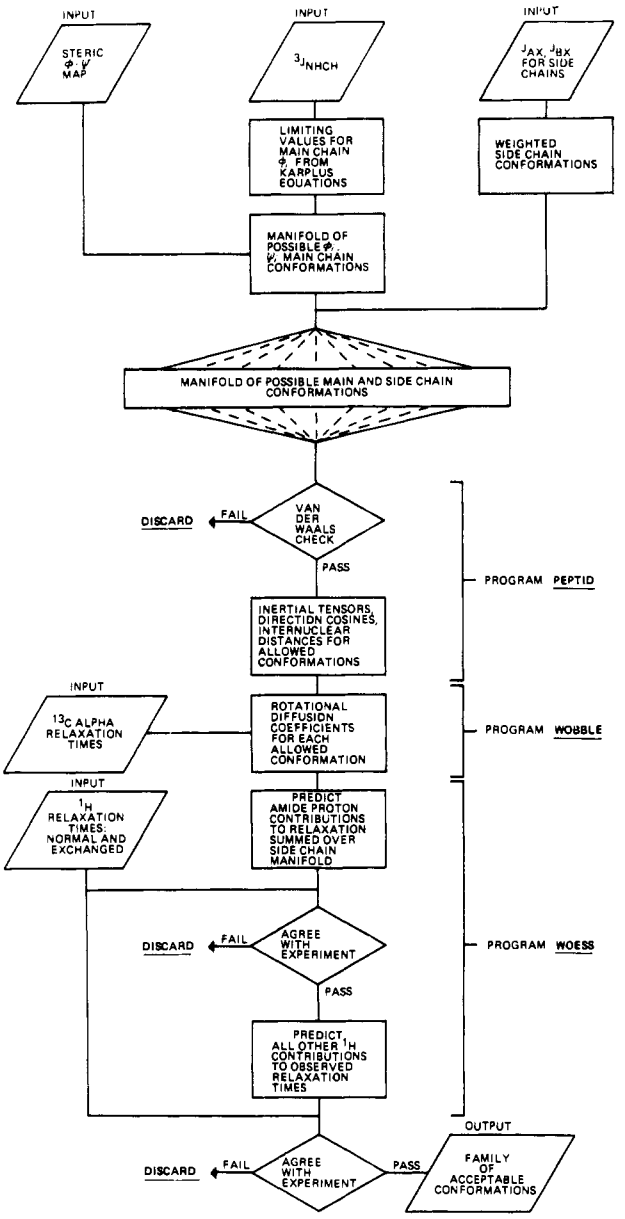

FIGURE 6: Flow diagram of the structural determination procedure used in this work.

The relaxation results from ^{13}C and ^1H experiments are then brought into play in the following manner. For each of the conformations, allowed on the grounds discussed above, rotational diffusion coefficients are determined by using WOBBLE. Given the trial conformation the ^{13}C relaxation rate for an α or formyl carbon is given in the general form

$$(1/T_1)_{^{13}C_i} = \frac{A}{r_{CH_i}^6} F(R_1,R_2,R_3,\omega_C,\omega_H,l_i,m_i,n_i) \quad (10)$$

where F is a sum of spectral density functions, as discussed above, A is a nuclear constant, r_{CH_i} is assumed known, and l_i, m_i, and n_i are vectorial direction cosines in the inertial system for the trial conformation. As already described, programs WOBBLE and PEPTID allow the set of diffusion coefficients to be derived from the set of experimental relaxation rates.

The amide exchange experiments allow us to immediately determine the *total* amide proton contribution to each observed nonexchangeable proton relaxation since

$$\begin{aligned}(1/T_1)_{\text{normal}} &= (1/T_1)_{\text{amide}} + (1/T_1)_{\text{others}} \\ (1/T_1)_{\text{exch}} &= (1/T_1)_{\text{others}} \\ (1/T_1)_{\text{normal}} - (1/T_1)_{\text{exch}} &= (1/T_1)_{\text{amide}}\end{aligned} \quad (11)$$

Then, for protons

$$\left(\frac{1}{T_1}\right)_{^1H,\text{amide}} = B\sum_{\substack{j,k \\ j\neq k}} \frac{F'jk(R_1,R_2,R_3,\omega_H,l_{jk},m_{jk},n_{jk})}{r_{jk}^6} \quad (12)$$

where r_{jk} is the internuclear proton–proton distance from the observed jth proton to the kth amide proton, F' is the sum of spectral densities associated with the set of diffusion coefficients for the particular conformation, l_{jk}, m_{jk}, and n_{jk} are the set of direction cosines for each dipolar interaction vector, and B is a nuclear constant. Bearing in mind the $1/r^6$ dependence, it is clear that the major contribution to a given proton's dipolar relaxation is mainly due to its closest proton neighbors.

For FMLP we proceed from the formyl end of the molecule. Reasons have been given above for assuming that the formyl proton–methionyl amide proton configuration is such that the two protons are cis with respect to one another. We use this fact as a filter to screen out conformations which would have this distance greater than it must be. If, for a given conformation, the predicted contribution to the formyl proton

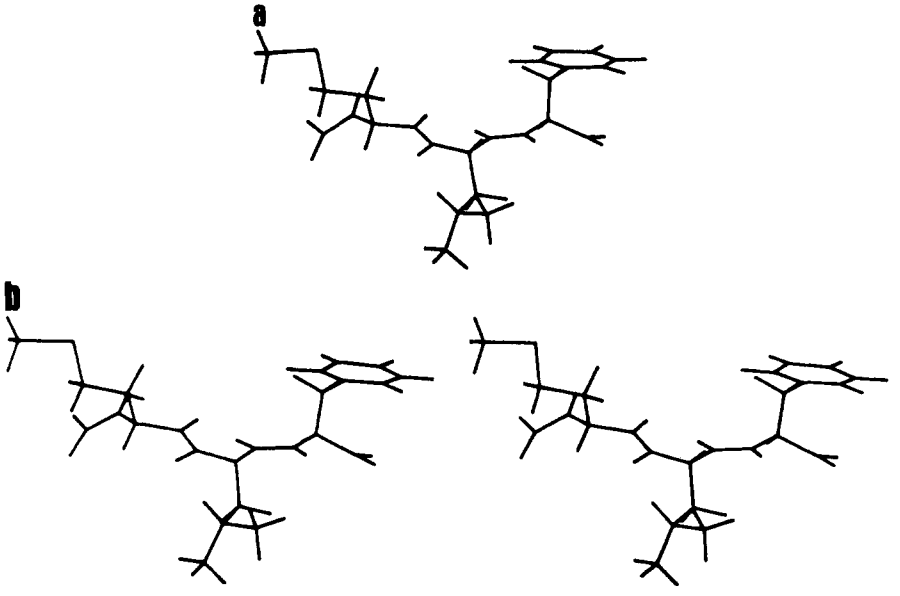

FIGURE 7: (a) Stick model of the most populated final structure. (b) Stereoimages stick model of the most populated final structure.

Table IX

Summed Amide Proton Contributions to Other Proton Spin–Lattice Relaxation Rates for f-Met-Leu-Phe-O$^-$, at 100 and 270 MHz, 30 °C, and Me_2SO-d_6

	100 MHz			270 MHz		
resonance	$1/T_{1,n}$ (s^{-1})	$1/T_{1,exch}$ (s^{-1})	% $1/T_{1,NH}$	$1/T_{1,n}$ (s^{-1})	$1/T_{1,exch}$ (s^{-1})	% $1/T_{1,NH}$
formyl	1.21 ± 0.04	0.392 ± 0.019	68 ± 4	0.731 ± 0.039	0.275 ± 0.010	62 ± 5
methionyl						
α	2.66 ± 0.20	1.51 ± 0.07	43 ± 8	1.68 ± 0.05	1.09 ± 0.04	35 ± 4
β_1[a]	3.57 ± 0.24	3.57 ± 0.24	0 ± 9	2.23 ± 0.19	3.42 ± 0.37	
β_2[a]				2.94 ± 0.16	4.12 ± 0.31	
γ	3.45 ± 0.09	2.80 ± 0.13	19 ± 5	2.72 ± 0.04	2.61 ± 0.10	20 ± 4
δ	0.752 ± 0.027	0.69 ± 0.03	8 ± 5	0.65 ± 0.62	0.649 ± 0.068	1 ± 10
leucyl						
α	2.72 ± 0.19	1.87 ± 0.07	31 ± 8	1.68 ± 0.04	1.34 ± 0.043	20 ± 4
β_1[a]	5.00 ± 0.30	5.13 ± 0.13	0 ± 7	4.12 ± 0.05	3.76 ± 0.30	
β_2[a]				4.25 ± 0.20	4.90 ± 0.40	
γ	3.57 ± 0.24	4.48 ± 0.26	0 ± 10	2.02 ± 0.08	1.75 ± 0.10	13 ± 6
δ_1	3.12 ± 0.08	3.08 ± 0.10	1 ± 4	2.65 ± 0.05	2.70 ± 0.14	0 ± 4
δ_2				2.56 ± 0.05	2.68 ± 0.10	0 ± 4
phenylalanyl						
α	1.74 ± 0.12	1.43 ± 0.06	18 ± 7	1.22 ± 0.03	0.992 ± 0.015	19 ± 3
β_1[a]	6.54 ± 0.36	7.14 ± 0.34		3.61 ± 0.16	3.88 ± 0.34	
β_2[a]				3.66 ± 0.32	4.29 ± 0.23	
aromatic	1.24 ± 0.10	1.24 ± 0.06	0 ± 16	0.85 ± 0.02	0.877 ± 0.037	0 ± 4

(a) Derived Rotational Diffusion Coefficients, for Family of Final Conformations
$\phi_1 = -130°$, $\psi_1 = 160°$, $\phi_2 = -120°$, $\psi_2 = 161°$, $\phi_3 = -150°$

conformation	R_1	R_2	R_3
P	$0.166 \times 10^{10} \pm 0.02$	$0.123 \times 10^{9} \pm 0.22$	$0.128 \times 10^{10} \pm 0.01$
O	$0.134 \times 10^{10} \pm 0.003$	$0.484 \times 10^{9} \pm 0.005$	$0.840 \times 10^{9} \pm 0.003$
K	$0.157 \times 10^{10} \pm 0.02$	$0.229 \times 10^{9} \pm 0.17$	$0.112 \times 10^{10} \pm 0.008$
J	$0.135 \times 10^{10} \pm 0.002$	$0.511 \times 10^{9} \pm 0.03$	$0.807 \times 10^{9} \pm 0.02$
R	$0.178 \times 10^{10} \pm 0.03$	$0.504 \times 10^{9} \pm 0.65$	$0.745 \times 10^{9} \pm 0.47$
S	$0.213 \times 10^{10} \pm 0.07$	$0.209 \times 10^{6} \pm 650$	$0.137 \times 10^{10} \pm 0.02$
T	$0.180 \times 10^{10} \pm 0.03$	$0.485 \times 10^{9} \pm 0.65$	$0.767 \times 10^{9} \pm 0.47$
X	$0.174 \times 10^{10} \pm 0.04$	$0.448 \times 10^{9} \pm 0.67$	$0.816 \times 10^{9} \pm 0.50$
Y	$0.223 \times 10^{10} \pm 0.11$	$0.735 \times 10^{5} \pm 10\,000$	$0.134 \times 10^{10} \pm 0.04$
Z	$0.188 \times 10^{10} \pm 0.02$	$0.527 \times 10^{9} \pm 0.40$	$0.711 \times 10^{9} \pm 0.26$

(b) Example of Derived Rotational Diffusion Coefficients, for Family of Conformations Differing from Final Conformation by a Slight Backbone Twist
$\phi_1 = -130°$, $\psi_1 = 160°$, $\phi_2 = -135°$, $\psi_2 = 120°$, $\phi_3 = -150°$

conformation	R_1	R_2	R_3
P	$0.156 \times 10^{10} \pm 0.005$	$0.159 \times 10^{9} \pm 0.053$	$0.117 \times 10^{10} \pm 0.003$
O	$0.106 \times 10^{10} \pm 0.037$	$0.417 \times 10^{9} \pm 0.760$	$0.970 \times 10^{9} \pm 0.520$
K	$0.132 \times 10^{10} \pm 0.048$	$0.351 \times 10^{9} \pm 0.426$	$0.926 \times 10^{9} \pm 0.300$
J	$0.105 \times 10^{10} \pm 0.040$	$0.475 \times 10^{9} \pm 0.786$	$0.880 \times 10^{9} \pm 0.550$
R	$0.274 \times 10^{10} \pm 0.053$	$0.142 \times 10^{10} \pm 0.470$	$0.65 \times 10^{5} \pm 3$
S	$0.203 \times 10^{10} \pm 0.039$	$0.155 \times 10^{9} \pm 0.320$	$0.107 \times 10^{10} \pm 0.020$
T	$0.173 \times 10^{10} \pm 0.230$	$0.164 \times 10^{10} \pm 0.380$	$0.490 \times 10^{5} \pm 5$
X	$0.851 \times 10^{9} \pm 5$	$0.237 \times 10^{9} \pm 46$	$0.135 \times 10^{10} \pm 3 \times 3$
Y	$0.202 \times 10^{10} \pm 0.002$	$0.171 \times 10^{9} \pm 0.002$	$0.107 \times 10^{10} \pm 0.001$
Z	$0.180 \times 10^{10} \pm 0.120$	$0.116 \times 10^{10} \pm 0.420$	$0.255 \times 10^{9} \pm 2.48$

[a] Multiplet; components differ between exchanged and nonexchanged spectra.

relaxation by the amide proton is not that observed, the conformation is discarded. Proceeding from the acceptable conformations by this criterion, we fit first the amide proton–α proton data to theory (by adjusting ϕ and ψ angles within the limits previously described). This is the first step since the exchange experiments present data bearing directly on this particular contribution. In more sophisticated experiments, now underway in our laboratory, specific deuteration at nonexchangeable positions is used to isolate proton pairs. We assume that for a given set of ϕ,ψ angles there is a manifold of 27 molecules, each characterized by a set of χ^1 angles. The analysis of the α–β spin multiplets which allows us to derive the rotamer populations of course assumes that interchange between rotamers takes place rapidly on the time scale characterized by $1/J_{AX}$ and $1/J_{BX}$, i.e., $\sim$ <0.03 s. This time scale is also rapid compared to the observed proton dipolar spin–lattice relaxation times and permits us to use the fast exchange limit for determining the relaxation rate for interchanging species (Zimmerman & Brittin, 1957) as

$$(1/T_1)_{obsd} = \sum_i \frac{P_i}{T_{1,i}} \qquad (13)$$

where P_i is the equilibrium population of the ith molecule and $T_{1,i}$ is its predicted relaxation time. The duration of time spent in each conformer must, on the grounds of simple reaction rate theory, be long compared to the rotational correlation time of the entire molecule. That is, we also assume that each of the 27 conformationally different molecules is characterized by a discrete set of rotational diffusion coefficients.

Our work is summarized in Tables IX and X where finally a large number of computer experiments are reduced to two examples. Table IX summarizes the results of observed amide proton contributions to the relaxation of other protons. In Table X is the matrix of derived rotational diffusion coefficient

Table X: Predicted and Observed Proton Relaxation Rates at 100 and 270 MHz and R Factors for Final Family of Conformations and Example Family

	$1/T_{1,100}$ (s^{-1}) obsd		$1/T_{1,270}$ (s^{-1}) obsd		Δ100	Δ270
Final Family						
α protons						
formyl	0.807	0.818	0.666	0.456	−0.011	+0.210
Met	1.134	1.150	0.924	0.590	−0.016	+0.334
Leu	1.014	0.850	0.857	0.340	+0.164	+0.517
Phe	0.269	0.310	0.187	0.228	−0.041	−0.041
R values: $R_{100} = 0.074$; $R_{270} = 0.683$						
amide protons						
Met	3.903	4.032	2.961	2.500	−0.129	+0.461
Leu	4.408	5.747	3.350	3.472	−1.339	−0.122
Phe	4.353	4.762	3.682	2.801	−0.410	+0.881
R values: $R_{100} = 0.129$; $R_{270} = 0.167$						
total R values: $R_{tot,100} = 0.119$; $R_{tot,270} = 0.247$						
Example Conformation						
α protons						
formyl	0.882	0.818	0.702	0.456	+0.064	+0.246
Met	1.264	1.150	0.972	0.590	+0.114	+0.382
Leu	2.048	0.850	1.630	0.340	+1.198	+1.290
Phe	0.261	0.310	0.185	0.228	−0.049	−0.043
R values: $R_{100} = 0.670$; $R_{270} = 1.215$						
amide protons						
Met	3.815	4.032	3.034	2.500	−0.217	0.534
Leu	4.184	5.747	3.304	3.472	−1.563	−0.168
Phe	4.739	4.762	3.767	2.801	−0.023	0.966
R values: $R_{100} = 0.124$; $R_{270} = 0.190$						
total R values: $R_{tot,100} = 0.183$; $R_{tot,270} = 0.349$						

values for two different main-chain conformations: (1) our final best fit and (2) a random example conformation differing from (1) by a rotation of ϕ_2 by −15° and ψ_2 by +41° (i.e., a small backbone twist). Table X thus shows the reflection of these values in the predicted relaxation times.

We define an "R" value, in analogy to other structural work, as

$$R = \frac{\sum^{\text{observations}} |(1/T_1)_{\text{theory}} - (1/T_1)_{\text{obsd}}|}{\sum (1/T_1)_{\text{obsd}}} \qquad (14)$$

in order to estimate the fit of theory to experiment. R values are shown in Table X for the two conformations. Close examination of Table X shows the conformational sensitivity of the predicted T_1's for α protons. The differences between experiment and theory for the amide protons are all in one direction. This indicates a slightly incorrect value of the nitrogen–proton distance which, however, we have not chosen to correct arbitrarily.

We are not able to comment on the slightly higher R values for 270-MHz measurements except to note that the instrument we were using did not have a correction device to minimize pulse defects (Cutnell et al., 1976), and therefore the data could be subject to small systematic error.

We note that despite the necessary complexity of this treatment we cannot rule out the possibility of other structures, consistent with the data, which eluded our search procedure. We emphasize that we searched only in regions of highly probable structures with initial grids of the order of ±20°. We are at present automating the computer procedures to provide uniform grid searches.

Conclusions

Our basic conformational finding is that the backbone of this chemotactic tripeptide is, to close approximation, consistent with the form of an antiparallel β sheet in the negatively charged form we have examined. In addition, the conformational manifold consists of a family of 10 major conformers differing from one another by their side-chain rotamer populations. The rotational motion of the molecule in solution is highly anisotropic for all of the members of the manifold although the *average* rotational diffusion coefficient over the manifold is relatively constant. The lifetimes of each side-chain conformer have not been studied in detail. This requires another form of measurement (Bleich & Glasel, 1978), spin–lattice relaxation in the rotating frame, which is sensitive to these motions. While we observe a low temperature coefficient for one of the amide proton chemical shifts, the family of conformations we derive has no features which can be directly responsible for this.

Because of the presence of the low chemical shift temperature coefficient exhibited by the phenylalanyl amide proton, we immediately suspected a conformation in the form of a 4 → 1 "β-turn" (Chandrasekaran et al., 1973). However, this must be ruled out because (a) the $^3J_{NHCH}$ for the methionyl residue is 3–4 times larger than would be predicted for a type I turn (and both are too high by this amount for a type II turn) and (b) the relaxation times predicted for the β-turn structures have very large R values. Other common structures such as completely elongated and α-helical backbones were examined and ruled out from relaxation data.

The chemotactic peptide under investigation here is obviously a very hydrophobic entity and is insoluble in water in the uncharged state. Therefore, it is perhaps not completely surprising that, in common with longer chain peptides of this nature, it is stabilized in the form of an antiparallel β structure. However, we are aware that the concept of a peptide *monomer* in a β-sheet conformation is not the usual picture. Despite this, ^{13}C T_1's and the results of PEPTID and WOBBLE combined with the Perrin equations (Perrin, 1934) show clearly that the rotational unit we are observing can only be a monomer. As discussed above we also measured ^{13}C chemical shifts as a function of concentration over the limited dilution range available to NMR spectroscopy and found no evidence of aggregation.

The explanation of why a molecule with an obvious tendency to aggregate does not do so may perhaps lie in the denaturing properties of the particular solvent system we are using. If so, it is entirely possible that in very dilute aqueous solutions (used in bioassays and achieved in practice only by first solubilizing FMLP in dimethyl sulfoxide) dimerization may be important.

It is interesting to compare our solution side-chain conformations to those found for the same residues in a variety of proteins and peptides in the solid state (Table VII). Our methionyl χ^1 structure does not correlate well with rotamer populations found in solids. However, for both the leucyl and phenylalanyl residues there is a remarkable correlation between the conformer populations found in a variety of materials in the solid state and our findings for FMLP in solution. This is especially apparent for leucine and may represent a conformational determinant in leucine-containing peptides.

Our proposed structure may have biological implications, if binding constant and activity are related, since it is known that a large decrease (factor of 10^4) in activity results when the formyl group is replaced by an amino terminus (Showell et al., 1976). If the binding of the chemotactic peptide to receptor is via the aligned hydrogen-bond donors (or acceptors) available in the structure proposed here, the loss of one such group, due to loss of the formyl moiety, would result in a free-energy loss corresponding to a drop in the binding

equilibrium constant by a factor of 10^4. We are currently testing this hypothesis by synthesizing analogues in which hydrogen-bond donors or acceptors are blocked.

Acknowledgments

We acknowledge the help of Drs. E. Schiffmann and H. Showell (for bioassays), Christine Regula (for technical assistance), and Mark Latina (for computer programming).

References

Aswanikumar, S., Corcoran, B., Schiffmann, E., Day, A. R., Freer, R. J., Showell, H. J., Becker, E., & Pert, C. (1977) *Biochem. Biophys. Res. Commun. 74*, 810.

Barfield, M., & Gearhart, H. L. (1973) *J. Am. Chem. Soc. 95*, 641.

Barry, C. D., Glasel, J. A., Williams, R. J. P., & Xavier, A. V. (1974) *J. Mol. Biol. 84*, 471.

Benedetti, E. (1977) in *Peptides* (Goodman, M., & Meinhofer, J., Eds.) p 257, Wiley, New York.

Berger, S., Kreissl, F. R., Grant, D. M., & Roberts, J. D. (1975) *J. Am. Chem. Soc. 97*, 1805.

Bleich, H. E., & Glasel, J. A. (1978) *Biopolymers 17*, 2445.

Bleich, H. E., Cutnell, J. D., & Glasel, J. A. (1976) *Biochemistry 15*, 2455.

Bleich, H. E., Day, A. R., Freer, R. J., & Glasel, J. A. (1977) *Biochem. Biophys. Res. Commun. 74*, 592.

Bleich, H. E., Easwaran, K. R. K., & Glasel, J. A. (1978) *J. Magn. Reson. 31*, 517.

Bleich, H. E., Glasel, J. A., Latina, M., & Visintainer, J. (1979) *Biopolymers* (in press).

Bystrov, V. F., Portnova, S. L., Tsetlin, V. I., Ivanov, V. T., & Ovchinnikov, Yu. A. (1969) *Tetrahedron 25*, 493.

Bystrov, V. F., Ivanov, V. T., Portnova, S. L., Balashova, T. A., & Ovchinnikow, Yu. A. (1973) *Tetrahedron 29*, 873.

Bystrov, V. F., Arsenieu, A. S., & Gaurilov, Yu. D. (1978) *J. Magn. Reson. 30*, 151.

Chandrasekaran, R., & Ramachandran, G. N. (1970) *Int. J. Protein Res. 2*, 223.

Chandrasekaran, R., Lakshminarayanan, A. V., Pandya, U. V., & Ramachandran, G. N. (1973) *Biochim. Biophys. Acta 303*, 14.

Chen, C. S., & Parthasarathy, R. (1977) *Acta Crystallogr., Sect. B 33*, 3332.

Chidambaram, R., Balasubramanian, R., & Ramachandran, G. N. (1970) *Biochim. Biophys. Acta 221*, 182.

Cody, V., Duax, W. L., & Hauptman, H. (1973) *Int. J. Pept. Protein Res. 5*, 297.

Cowburn, D., Fischman, A. J., Live, D. H., Agosta, W. C., & Wyssbrod, H. R. (1977) in *Peptides* (Goodman, M., & Meinhofer, J., Eds.) p 322, Wiley, New York.

Cung, M. T., Marraud, M., & Neel, J. (1974) *Macromolecules 7*, 606.

Cutnell, J. D., Bleich, H. E., & Glasel, J. A. (1976) *J. Magn. Reson. 21*, 43.

Day, A. R., & Freer, R. J. (1979) *Int. J. Pept. Protein Res.* (in press).

Day, A. R., Radding, J. A., Freer, R. J., Showell, H. J., Becker, E. L., Schiffmann, E., Corcoran, B., Aswanikumar, S., & Pert, C. (1977) *FEBS Lett. 77*, 291.

Fischman, A. J., Wyssbrod, H. R., Agosta, W. C., & Cowburn, D. (1978) *J. Am. Chem. Soc. 100*, 54.

Gibbons, W. A., Nemethy, G., Stern, A., & Craig, L. C. (1970) *Proc. Natl. Acad. Sci. U.S.A. 67*, 239.

Glickson, J. D., Gordon, S. L., Pitner, T. P., Agresti, D. G., & Walter, R. (1976) *Biochemistry 15*, 5721.

Gupta-Bhaya, P. (1975) *Biopolymers 14*, 1143.

Hallenga, K., & Van Binst, G. (1979) *Biochim. Biophys. Acta* (in press).

Hayashi, F., Akasaka, K., & Hatano, H. (1977) *J. Magn. Reson. 27*, 419.

IUPAC–IUB Commission (1970) *J. Biol. Chem. 245*, 6489.

Janin, J., Wodak, S., Levitt, M., & Maigret, B. (1978) *J. Mol. Biol. 125*, 357.

Karplus, M. (1963) *J. Am. Chem. Soc. 85*, 2870.

Khaled, M. A., & Urry, D. W. (1976) *Biochem. Biophys. Res. Commun. 70*, 485.

Kimmich, R. (1977) *Z. Naturforsch., A 32*, 544.

Koetzle, T. F., Hamilton, W. C., & Parthasarathy, R. (1972) *Acta Crystallogr., Sect. B 28*, 2083.

Leach, S. J., Nemethy, G., & Scheraga, H. A. (1977) *Biochem. Biophys. Res. Commun. 75*, 207.

Mitra, A. K. (1978) *Int. J. Pept. Protein Res. 11*, 166.

Perrin, F. (1934) *J. Phys. Radium 5*, 497.

Pople, J. A., Schneider, W. G., & Bernstein, H. J. (1959) *High-Resolution Nuclear Magnetic Resonance*, McGraw-Hill, New York.

Ramachandran, G. N., Chandrasekaran, R., & Kopple, K. D. (1971) *Biopolymers 10*, 2113.

Robin, M. B., Bovey, F. A., & Basch, H. (1970) in *The Chemistry of the Amides* (Zabicky, J., Ed.) p 1, Interscience, New York.

Schiffmann, E., Corcoran, B. A., & Wahl, S. M. (1975) *Proc. Natl. Acad. Sci. U.S.A. 72*, 1059.

Schroeder, R., & Lippincott, E. R. (1957) *J. Phys. Chem. 61*, 921.

Showell, H. J., Freer, R. J., Zigmond, S. H., Schiffmann, E., Aswanikumar, S., Corcoran, B., & Becker, E. L. (1976) *J. Exp. Med. 143*, 1154.

Thong, C. M., Canet, D., Grenger, P., Marraud, M., & Neel, J. (1969) *C. R. Hebd. Seances Acad. Sci., Ser. C 269*, 580.

Tilak, M. A. (1970) *Tetrahedron Lett. 11*, 849.

Weinkam, R. J., & Jorgensen, E. C. (1971) *J. Am. Chem. Soc. 93*, 7038.

Wilkinson, P. C. (1974) *Chemotaxis and Inflammation*, Churchill-Livingstone, London.

Woessner, D. E. (1962) *J. Chem. Phys. 37*, 647.

Zimmerman, J. R., & Brittin, W. E. (1957) *J. Phys. Chem. 61*, 1328.